Journal of the Korean Magnetic Resonance Society **2023**, *27*, 23-27
DOI 10.6564/JKMRS.2023.27.4.023

Backbone assignment of human Hoxc9DBD

Ja-Shil Hyun and Sung Jean Park*

College of Pharmacy and Gachon Institute of Pharmaceutical Sciences, Gachon University, 191 Hambakmo-ero, Yeonsu-gu, Incheon 21936, Republic of Korea

Received Nov 20, 2023; Revised Dec 04, 2023; Accepted Dec 04, 2023

Abstract Hoxc, or the Homeobox C cluster, is a group of genes that play a crucial role in embryonic development, particularly in patterning the body along the anterior-posterior axis. These genes encode transcription factors, which are proteins that bind to DNA and regulate the expression of other genes. Hoxc9 is specifically involved in the development of the skeletal system, nervous system, and adipose tissue. Hoxc9 overexpression has been linked to the development of various cancers such as leukemia and breast cancer. Here, we assigned the chemical shifts Hoxc9 DNA binding domain (DBD) using heteronuclear NMR techniques. The helical regions of Hoxc9 DBD correspond to the residues T200 – F213 (Helix I), T218 – L229 (Helix II), and T232 – K249 (Helix III). Our result would be helpful for studing the molecular interactions of the Hoxc9 DBD and other proteins.

Keywords Backbone assignment, Hoxc9, NMR, Triple resonance

Introduction

Hoxc9 DBD is the DNA binding domain of the Hoxc9 protein. It is a homeodomain, which is a type of DNA-binding protein that plays a critical role in development.[1] Hoxc9 DBD is involved in regulating the expression of genes that are important for patterning the body,[2] and it has been shown to be involved in a number of developmental processes, including limb development,[3] hindbrain development, and hematopoiesis.[4]

Hoxc9 DBD is a key regulator of development, and it has been implicated in a number of developmental disorders. Mutations in the Hoxc9 gene have been found to cause a number of skeletal defects,[5] including synpolydactyly (extra fingers or toes), and mutations in the Hoxc9 gene have also been found to be associated with a number of cancers, including leukemia[6] and lymphoma.[7] Hoxc9 expression is increased in adipose tissue from obese individuals. It is thought to contribute to obesity by promoting adipocyte differentiation and fat storage.[8]

Hoxc9 DBD is a relatively small protein, consisting of around 60 amino acids. It is composed of three helices and a loop, and it binds to DNA through a recognition helix that inserts into the major groove of the DNA double helix.[9] Hoxc9 DBD has been shown to bind to a number of different DNA sequences, and its binding specificity is determined by a number of factors, including the sequence of the DNA and the presence of other proteins.

The chemical shifts of the homeodomain of Hoxc9 complexed with the cell cycle regulator Geminin was reported previously[10] while there is no information of apo Hoxc9s. Here, we report the sequence-specific backbone resonance assignments of the apo Hoxc9 DBD.

* Address correspondence to: **Sung Jean Park,** College of Pharmacy and Gachon Institute of Pharmaceutical Sciences, Gachon University, 191 Hambakmo-ero, Yeonsu-gu, Incheon 21936, Republic of Korea, Tel: 82-32-820-4957; E-mail: psjnmr@gachon.ac.kr

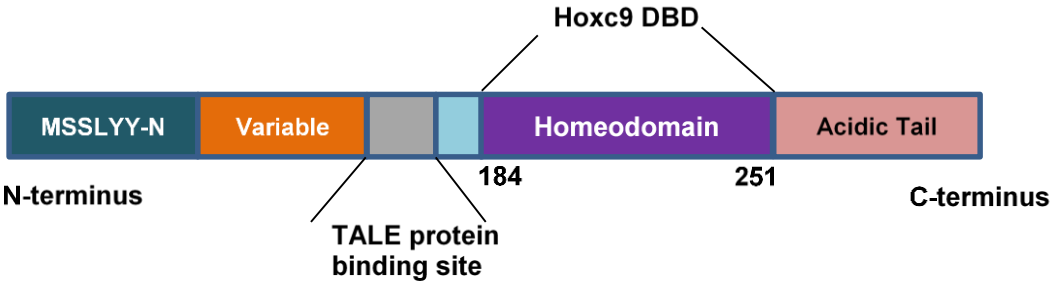

Figure 1. Domain composition of Hoxc9. Hoxc9DBD (DNA binding domains) for NMR studies consists of residues 184 to 241.

Experimental Methods

Sample preparation- The gene that encodes human Hoxc9 DBD was inserted into the pET28a vector using the Ncol and Xhol sites. The construct was transformed into Resetta2 (DE3) *Escherichia coli*. The *E. coli* cells were grown in luria bertani (LB) media at 37 degree until the OD_{600} was 0.5, and then isopropyl-β-D-1-thiogalactopyranoside (IPTG) was added to a final concentration of 0.5mM. Cells were harvested 16h after induction at 20℃. Cells were harvested and resupended in the buffer. Cells were sonicated and centrifugated to remove the cell debris. Hoxc9 DBD was purified by cation exchange chromatography with HiTrapTM SP HP (GE healthcare) and followed by and gel filtration chromatography with Hiprep 26/60 sephacryl S100 (GE healthcare). To prepare uniformly ^{15}N-labeled Hoxc9 DBD, bacterial cells were cultured in M9 minimal medium containing 99% $^{15}NH_4Cl$ (Cambridge isotope laboratories, Inc.) The ^{15}N-labeled proteins were dissolved in 20mM sodium phosphate buffer (pH6.5) containing 10% D_2O and 50mM NaCl, 1mM EDTA. For preparing the triply [^{15}N, ^{13}C, and ^{2}H]-labeled Hoxc9 DBD, two liter cultures of the transformed *E.coli* were grown in M9 media with ^{15}N ammonium chloride as the nitrogen source and ^{13}C glucose as the carbon source and 70% D_2O instead of H_2O.

NMR experiments- Backbone and side chain ^{1}H, ^{13}C and ^{15}N resonances for Hoxc9 DBD were assigned based on standard triple-resonance experimental spectra. Sequential assignment of ^{13}C, ^{15}N-labeled proteins was achieved by 3D triple resonance through-bond scalar correlation experiments such as 3D HNCO, HNCACO, HNCA, HN(CO)CA, HNCACB, CBCA(CO)NH experiments[19,20] Two dimensional ^{1}H,^{15}N-HSQC spectra were recorded with uniformly ^{15}N-labeled Hoxc9 DBD. All NMR experiments were performed at 298K on a Bruker AVANCE DRX 600 and 800 MHz spectrometer equipped with a cryogenic probe. NMR data were processed using NMRPipe and analyzed using NMRView. Protein samples for NMR experiments were prepared in NMR buffer (20mM sodium phosphate buffer, 50mM NaCl and 1mM EDTA, pH6.5).

Secondary Structure Estimation- The secondary structure was determined from the ^{1}H and ^{13}C chemical shift values, using the CSI program.[11] A combination of four kinds ($^{1}H_\alpha$, $^{13}C_\alpha$, $^{13}C_\beta$, and $^{13}C'$) of chemical shifts was used for CSI prediction. The consensus mark '1' represents the β-strand tendency of the atom of the residue (upfield shifts of $13C_\alpha$ or 13C′ resonances, and downfield shifts of $13C_\beta$ resonances from their reference values), while the consensus mark '-1' represents the α-helical tendency. The chemical shift within the reference value range was marked as a '0', which means random-coil tendency. For estimation of backbone dihedral angles, TALOS method was used to calculate angles, based on the chemical shifts.[12]

Results and Discussion

Backbone assignment of Hoxc9 DBD– . The ^{1}H, ^{15}N-HSQC spectrum of ^{15}N-enriched HMGB1 A-box showed well-dispersed cross-peaks, indicating that the overall structure of the Hoxc9 DBD is well defined.

theose of the isolated prolines. The available resonances is depicted in Figure 2.

Secondary Structure Estimation- As like the CD study (data not shown), Hoxc9 DBD adopts a helical structure. To clearly identify the secondary structural

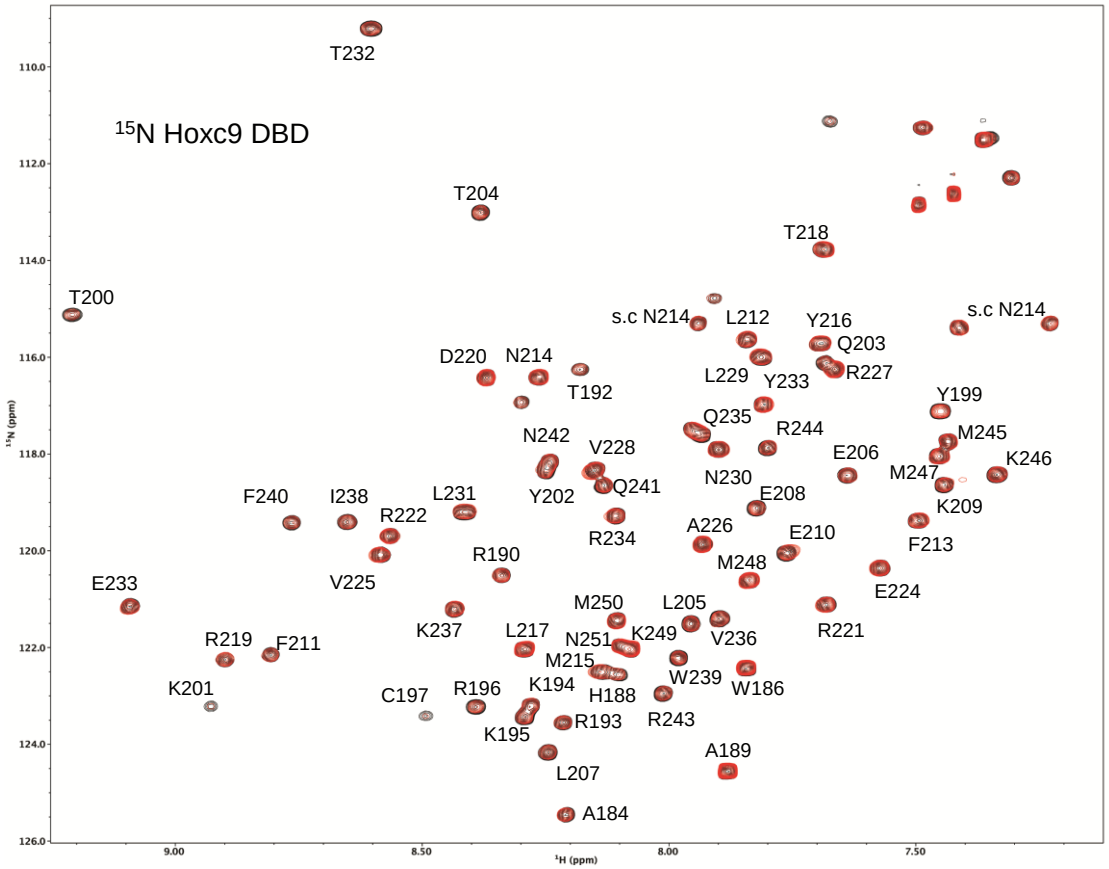

Figure 2. Two dimensional [^{1}H, ^{15}N]-HSQC spectra of Hoxc9 DBD. The assigned residues are depicted with the residue numbers.

Most of the ^{1}HN, ^{15}N, ^{13}Cα, ^{13}Cβ, and ^{13}CO resonance assignments were obtained from analyses of the 3D HNCA, HNCACB, CBCA(CO)NH, HN(CA)CO and HNCO spectra.[13] Since any one residue manifests the same HN and ^{15}N chemical shift signals in each spectrum, the related peaks could be combined into a peak cluster. The backbone amide resonances for 65 possible residues were completely assigned, except for

composition, we determined the secondary structure using assigned backbone chemical shifts. The CSI (Chemical Shift Index) approach,[14] which is fundamentally a statistical technique, was developed to provide a NOE-independent method for structure determination. The CSI results of Hoxc9 DBD revealed a patterned distribution of the marks -1, 0, and 1, with consensus values, which indicated that the Hoxc9 DBD consists of three helices. These helices to the residues T200 – F213 (Helix I), T218 – L229

(Helix II), and T232 – K249 (Helix III), which is depicted in figure 3. This result is almost consistent with the TALOS prediction (Fig. 3) that represents the backbone dihedral angles, φ and ψ.

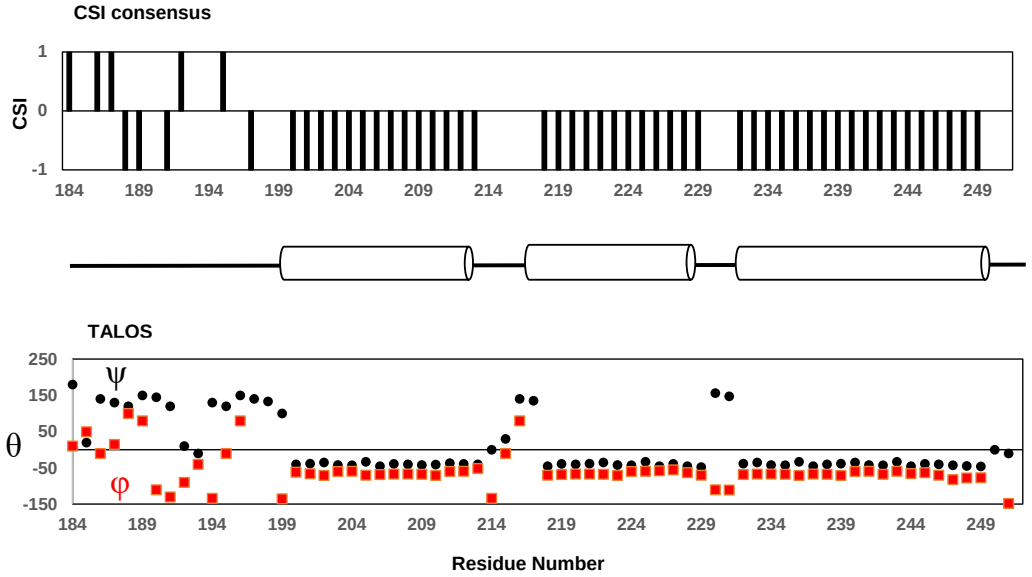

Figure 3. Summary of structural information obtained from NMR spectra. The CSI values of each residue for H_α, C_α, CO, and C_β are obtained and the consensus values are depicted. The negative vertical bars indicate helical region in the consensus CSI diagram. The schematic representation of the secondary structure of Hoxc9 DBD. The cylinders represent the helices. (c) φ and Ψ angle values are predicted by TALOS. The filed rectangles represent the backbone φ angles and the filed circles the backbone Ψ angles.

In general, a right handed helical structure shows the average torsion angles φ = -60 and ψ = -40. The averages of the torsion angles (φ, ψ) obtained in the helical regions of the proteion were -62.1 ± 5.0, -40 ± 3.5 (Helix I), -68.3 ± 10.4, -37.0 ± 9.2 (Helix II), and -72.1 ± 7.4, -32.1 ± 10.1 (Helix III) respectively, which are well consistent with the typical helical propensity (Note that the values used in this average calculation were involved in the class that TALOS classified as 'good'.). Taken together, the results of CSI and TALOS suggest the Hoxc9 DBD adopts highly helical structure with three helices..

Conclusion

Based on the NMR titration results, the expected apo structure of Hoxc9DBD (Fig. 3) was obtained. The N terminal loop region of Hoxc9DBD may interact with various proteins. In this study we assigned the chemical shifts of apo Hoxc9DBD, which may be helpful for studying various interactions and give a good tool to discover binding chemicals.

Acknowledgements

This work was supported by grants from the National Research Foundation of Korea (NRF-2021R1F1A1061607 and 2020R1A6A1A0304370812).

References

1. S. J. Stoll, S. Bartsch, H. G. Augustin, J. Kroll, *Circ. Res*. **108**, 1367 (2012)
2. S. J. Stoll, S. Bartsch, J. Kroll, *PLoS One* **8**, e58311 (2013)
3. R. Sheth, M. F. Bastida, M. Ros, *Dev. Biol*. **310**, 430 (2007)
4. M. C. Magli, C. Largman, H. J. Lawrence, *J. Cell Physiol*. **173**, 168 (1997)
5. H. Suemori, N. Takahashi, S. Noguchi. *Mech. Dev*. **51265** (1995)
6. V. Dobrotkova, P. Chlapek, M. Jezova, K. Adamkova, P. Mazanek, J. Sterba, R. Veselska, *PLoS One* **14**, e0218269 (2019)
7. J. Xu, H. Huang, S. Wang, Y. Chen, X. Yin, X. Zhang, Y. Zhang, *Arch. Dermatol. Res*. **312**, 513 (2020)
8. J. E. Brune, M. Kern, A. Kunath, G. Flehmig et al., *Obesity (Silver Spring)* **24**, 51 (2016)
9. H. H. Kim, S. J. Park, J. H. Han, C. Pathak, H. K. Cheong, B. J. Lee. *Biochim. Biophys. Acta* **1854**, 449 (2015)
10. B. Zhou, C. Liu, G. Zhu, *Biomol. NMR Assign* **9**, 165 (2015)
11. D. S. Wishart and A. M. Nip, Biochem. *Cell. Biol*. **76**, 153 (1998)
12. G. Cornilescu, F. Delaglio, and A. Bax, *J. Biomol. NMR*. **13**, 289 (1999)
13. J. W. Choi and S. J. Park, *J. Kor. Magn. Reson. Soc.* **25**, 17 (2021)
14. M. J. Yang and C. Park, *J. Kor. Magn. Reson. Soc.* **27**, 17 (2023)